Holographic interference, filters for infrared communications

Diehl, D.W.; George, N.

published in
Applied Optics
2003

DOI (link to publisher)
10.1364/AO.42.001203

document version
Publisher's PDF, also known as Version of record

Holographic interference filters for infrared communications

Damon W. Diehl and Nicholas George

We demonstrate that high-quality interference filters for the wavelength range 1300–1600 nm can be holographically fabricated in DuPont HRF-800X001 photopolymer material by use of visible laser illumination. We also summarize a chain-matrix technique, which we call thin-film decomposition, that is useful for modeling multilayer films with an arbitrary index profile $n(z)$. We use the thin-film-decomposition technique to create design curves that allow one to choose the proper exposure angle and film thickness with which to fabricate a holographic interference filter with a desired transmission efficiency and bandwidth at a particular wavelength. These curves are of general utility and are not confined to any particular holographic recording medium. Excellent agreement between theory and experiment is found. © 2003 Optical Society of America

OCIS codes: 060.4510, 090.0090, 350.2460, 090.2890, 090.4220, 090.2900.

1. Introduction

Photopolymer materials offer attractive possibilities for use in the holographic fabrication of multilayer interference filters for infrared wavelengths; of particular interest are multitone filters with reflection bands at multiple wavelengths. Such filters are useful in optical communications applications. In this paper we demonstrate, through both theory and experiments, a technique for fabricating multitone interference filters for the wavelength range 1300–1600 nm, using visible wavelengths for the exposure.

It has long been known that one can produce highly efficient holographic mirrors by recording the interference of counterpropagating laser beams within a high-resolution photographic film. For early literature on this field, the reader is directed to a publication of collected reprints.[1] Of particular interest is the possibility of using a total internal reflection system to record infrared mirrors by using visible laser illumination.[2,3] Such mirrors have wavelength selection properties and bear a striking resemblence to rugate filters in which the index of refraction varies in a continuous, corrugated manner along the direction of propagation. A comprehensive history of the theory of inhomogeneous films has been compiled by Jacobsson.[4]

Photopolymer materials were first used for holography in 1969.[5] Since then, commercial classes of photopolymer have been introduced by Polaroid[6] and by DuPont.[7] Index modulation strengths as high as $\Delta n = 0.2$ have been reported for Polaroid's DMP-128 polymer, which has been used to develop high-quality infrared multilayers for eye-hazard protection at 1.06 μm.[3] Initially an important material for high-quality mirrors at 1.06 μm was dichromated gelatin. A comparison of the quality of holographic notch filters for visible wavelengths recorded in dichromated gelatin and in DuPont photopolymer has been made.[8] It is difficult to protect dichromated gelatin in an application environment in which humidity is a problem. Information relative to modulation profiles of gratings recorded in dichromated gelatin has been reported in the literature.[9] An important advance in photopolymer technology was DuPont's development of a material that is sensitized over the entire visible spectrum and thus is suitable for full-color holography.[10] Broadband multitone multilayer mirrors for visible wavelengths have been recorded in this material.[11] Furthermore, methods to characterize the index, shrinkage, and scattering of the DuPont photopolymer have been presented.[12,13] High reflectors fabricated from DuPont photopolymer are extremely efficient and are now found in enhanced reflective liquid-crystal displays.[14]

The authors are with The Institute of Optics, University of Rochester, Rochester, New York 14627-0186. D. W. Diehl's e-mail address is damon@optics.rochester.edu. N. George's e-mail address is ngeorge@troi.cc.rochester.edu.

Received 5 June 2002; revised manuscript received 11 October 2002.

0003-6935/03/071203-08$15.00/0

In Section 2 of this paper we describe the fabrication from DuPont HRF-800X001 photopolymer of holographic filters for operation in the wavelength range from 1300 to 1600 nm. The photopolymer requires exposure with visible wavelengths, which necessitates the use of the total internal reflection configuration mentioned above.[2,3] The holograms were measured with a conventional spectrophotometer. Using these data, we demonstrate that the DuPont HRF-800X001 photopolymer has low loss and low index dispersion in the near infrared. We also describe a scanning laser diode spectrophotometer that is useful for the characterization of infrared interference filters. It is calibrated by means of an acetylene absorption cell.[15]

In Section 3 we compile our experimental data into design curves that relate the exposure angle, hologram thickness, and index modulation required for fabrication of a holographic interference filter with a desired efficiency and bandwidth at a particular wavelength. To create these curves we use a computer-calculation technique, which we term thin-film decomposition. In thin-film decomposition, an inhomogeneous film is modeled as a stack of homogeneous layers, and each layer is characterized by a 2×2 matrix. The technique of thin-film decomposition has been used to model rugate filters[4] and more recently to model holographic multilayers.[16,17] The terminology "thin-film decomposition" is used in analogy to "thin grating decomposition," a similar technique in which a thick grating is treated as a cascade of thin gratings.[18–21]

2. Holographic Fabrication of Interference Filters

One fabricates a holographic multilayer mirror by recording the interference pattern created by two beams incident at equal angles from opposite sides of a film plate. For beams inclined from normal by an angle θ_f, the resulting index profile will vary only as a function of film depth, with a period Λ given by the equation

$$\Lambda = S \frac{\lambda_0}{2n_f(\lambda_0)\cos\,\theta_f}, \tag{1}$$

where S indicates the shrinkage of the film and $n_f(\lambda_0)$ is the average index of the film, before processing, at the exposure wavelength λ_0 as measured in free space. By varying either the exposure angle or the exposure wavelength, one may vary the period of the index modulation. A multilayer holographic mirror, with periods as described in Eq. (1), will have a reflection peak at the reconstruction wavelength (i.e., $\lambda = \lambda_p$) given by

$$\lambda_p = 2n_f'(\lambda_p)\Lambda\,\cos\,\theta_f', \tag{2}$$

where $n_f'(\lambda)$ is the average index of the postprocessed film at free-space wavelength λ and θ_f' is the angle of inclination of the reconstruction beam within the film.

A multitone filter is a holographic interference filter with two or more reflection peaks. We have explored two techniques for fabricating such a filter. The first technique involves making multiple exposures within a single layer of film, each with a different period. We term this an interleave filter. The second technique involves recording single holograms with different periods inside separate layers of film and then sandwiching the layers together. We term this a cascade filter.

For either type of hologram, one may control the period of the index modulation by adjusting the exposure wavelength or the exposure angle. Because the sensitivity of the DuPont photopolymer varies significantly with wavelength, it can be difficult to determine the optimal exposure time for multiple-wavelength exposures such that the final efficiencies of all the reflection tones will be equal. For this reason, in the experiments described in this paper we focus on varying the exposure angle.

Although the fabrication of multitone holograms is the final goal of this research, in this paper we describe the exposure techniques for fabricating single-tone holograms at a desired wavelength, with a desired bandwidth and efficiency. We intend to use these design curves in future research to fabricate multitone holographic interference filters.

Our objective for these experiments was to fabricate mirrors that reflect wavelengths in the range 1300–1600 nm when they are illuminated at normal incidence ($\theta_f' = 0$). Such a large period, Λ, requires that the recording beam angle, θ_f, be larger than the critical angle of the film–air interface. We therefore used a 45° roof prism to couple the TE-polarized beam into the film, as illustrated in Fig. 1. Total internal reflection at the film–air interface provides the second beam for our holographic exposures.[2,3] For the geometry shown, by using Snell's law we can write the following equations that relate the external angle of the beam, θ_i, to the angle within the film, θ_f:

$$\begin{aligned} n_p \sin\,\theta_1 &= n_0 \sin\,\theta_i, \\ \theta_2 &= 45° - \theta_1, \\ n_f \sin\,\theta_f &= n_p \sin\,\theta_2. \end{aligned} \tag{3}$$

The prism was made from Schott SF6 glass, which has an index of $n_p(590\text{ nm}) = 1.80518$. Such a high index ensured that light would couple into the film at an angle steep enough to create an index modulation of the desired large period. Were this system to be built anew, a suitable prism with an index more closely matched to the photopolymer could be used. However, in our experiments we did not experience undue reflections or parasitic gratings as a result of this index mismatch. The prism was mounted upon a Klinger rotation stage with a Heidenhain shaft encoder, allowing us to rotate the prism with a precision of 0.0001°. Our holograms were recorded with a Coherent Model 699-21 dye laser. Rhodamine 6G was used as the dye and permitted a tunable range of 560–620 nm. The laser was frequency stabilized to $\Delta\nu < 1$ MHz, and the wavelength was monitored by a

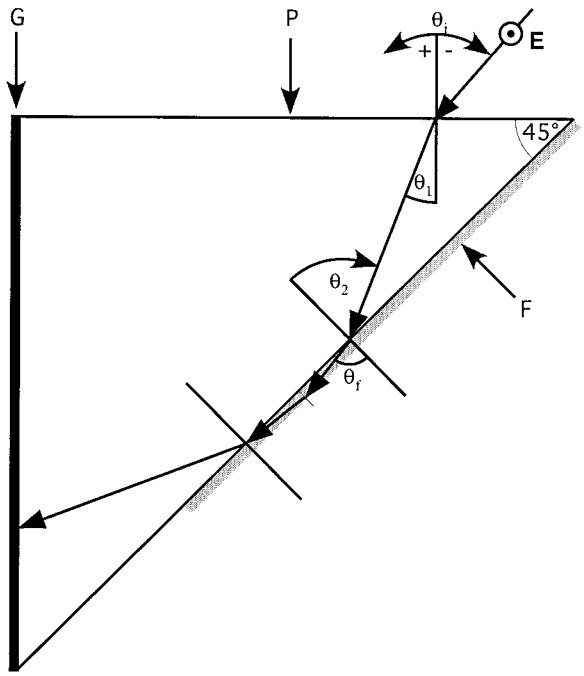

Fig. 1. Setup for holographic fabrication of infrared multilayer mirrors, showing the path of a ray through the prism–film assembly: F, film; P, 45° roof prism; G, black glass; **E**, electric field vector polarized perpendicular to the plane of incidence. Light is *s* polarized with respect to the prism face.

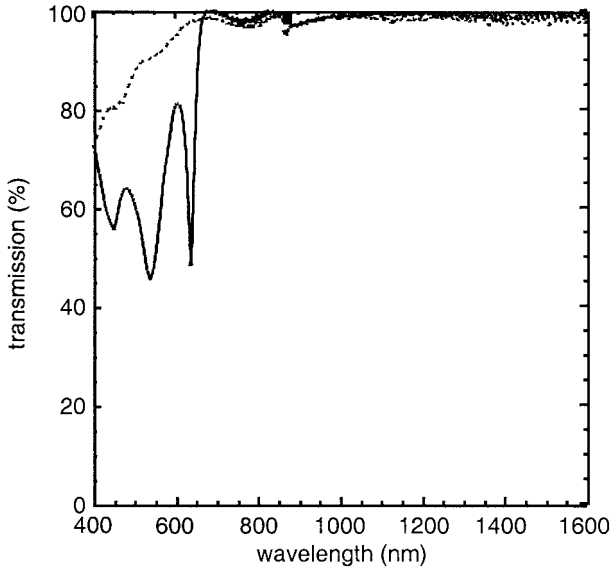

Fig. 2. Comparison of the transmission spectra through DuPont HRF-800X001-15 photopolymer film. Solid curve, before exposure; dashed curve, after polymerization.

Lasertechnics wavemeter with a resolution of 0.001 nm. The laser was tuned to $\lambda_0 = 590.0 \pm 0.1$ nm for all the exposures, and the beam was expanded, spatially filtered, and collimated. For all exposures, the power of the collimated beam was 1–2 mW/cm^2.

For these experiments we selected DuPont HRF-800X001-15 photopolymer film, which has a thickness of 15 μm. It has been determined that DuPont photopolymer has a shrinkage factor $S = 0.975 \pm 0.003$ and a preprocessed average index $n_f(632\text{ nm}) = 1.487 \pm 0.002$.[12] The DuPont HRF-800 × 001-15 photopolymer lies between two protective Mylar layers, one of which may be removed. We used an index-matching fluid of 1.67 to attach the Mylar–photopolymer sandwich to the prism. The thinner, removable layer of Mylar was attached to the prism.

To better understand the sensitivity of the DuPont photopolymer, we used a spectrophotometer to measure the transmission spectrum, before and after curing, over the range 400–1600 nm. These curves are shown in Fig. 2. As has been reported,[8] the photopolymer is absorptive (i.e., sensitive) to visible wavelengths; however, our curves show that it is essentially transparent (transmission greater than 95%) to infrared wavelengths of 1300–1600 nm. It is interesting to note that, over the visible spectrum, the photopolymer is most transparent (and thus least sensitive) to light near 590 nm, which is precisely the wavelength that we chose to use for our exposures. Although the lower sensitivity necessitates longer exposure times, it also means that the intensities of our interfering beams will be more nearly identical throughout the depth of the film, increasing the fringe contrast and better utilizing the available index modulation.

Exposures were made over a range of incident angles that varied from 0° to −10° (we used the sign convention shown in Fig. 1). Holograms were exposed until a fluence of 100 mJ/cm^2 within the film had been achieved. (This higher exposure energy was necessary because of the reduced film sensitivity at 590 nm.) In calculating the exposure times, which were of the order of 60 s, we took special care to account for Fresnel losses at the interfaces and the fall-off of power/area with the cosine of θ_f.

After exposure the thinner layer of Mylar was removed. A Kodak print roller was used to laminate the film, polymer side down, onto a float glass substrate, 1.7 mm thick. Following DuPont's instructions,[10] we cured the laminated plates, using broadband ultraviolet/white light, and then baked them for 2 h at 120 °C.

After cooling, the transmission spectra of the holograms were measured with a Perkin-Elmer spectrophotometer. Example spectra for four holograms are shown in Fig. 3.

One of our first interests was in characterizing the index dispersion of the DuPont HRF-800X001 photopolymer in the infrared range. Using our data and Eqs. (1)–(3), we calculated the average index of the photopolymer, n_f', as a function of replay wavelength λ. The results are plotted in Fig. 4. (The index modulation in the infrared, Δn, is described in Section 3 below.) We found no statistically significant variation in n_f' over the wavelength range 1300–1550 nm, implying that DuPont HRF-800X001 photopolymer has negligible index dispersion in the infrared range of interest. Disregarding data points beyond two standard deviations, we found the mean

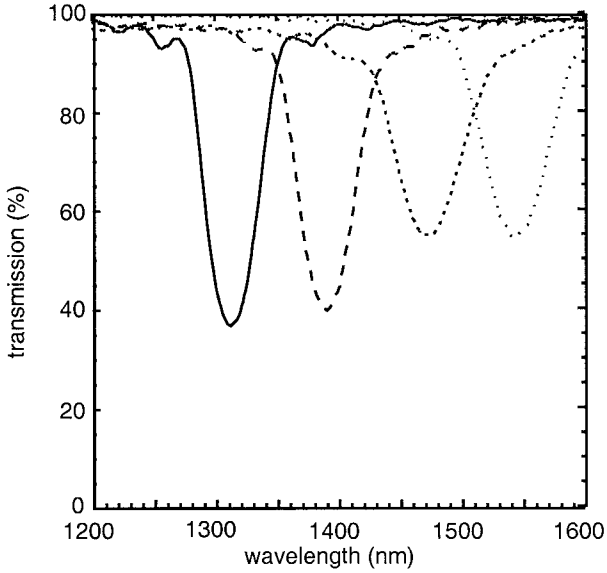

Fig. 3. Overlay of the transmission spectra of four holograms, showing reflection peaks at 1311, 1391, 1473, and 1541 nm.

value for n_f' to be 1.485 ± 0.005, as indicated by the dashed line in Fig. 4.

It became clear, over the course of our measurements, that one of the limiting factors in this experiment was the precision of the spectrophotometer. In most spectrophotometers (such as the Perkin-Elmer system used for these experiments) broadband radiation is filtered through a system of gratings to produce a beam of light with a wavelength that is tunable to a resolution of approximately 0.01 nm. This beam is then focused onto the surface of the test sample. The cone of the incident light can be as great as 10°. Such a beam is less than ideal for testing interference filters. There are two reasons for this. First, because the test beam comes from a thermal source with limited coherence length, interference features may be missed if the filter is thicker than the coherence length of the test beam. Second, because the behavior of interference filters is, in general, highly angle dependent, illuminating an interference filter with a cone of light will cause the features of the reflection spectra to be broadened and slightly blueshifted. This broadening and shifting will obscure narrow features.

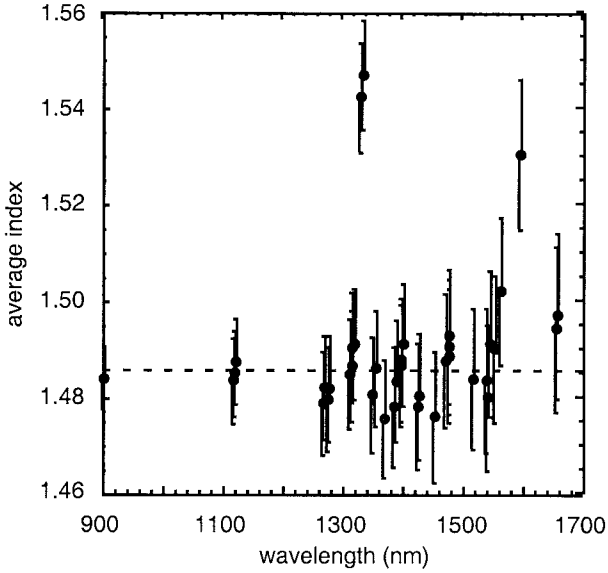

Fig. 4. Experimental data for the average index of refraction, n_f', of DuPont HRF-800X001 photopolymer after exposure and processing. Dashed line, mean value.

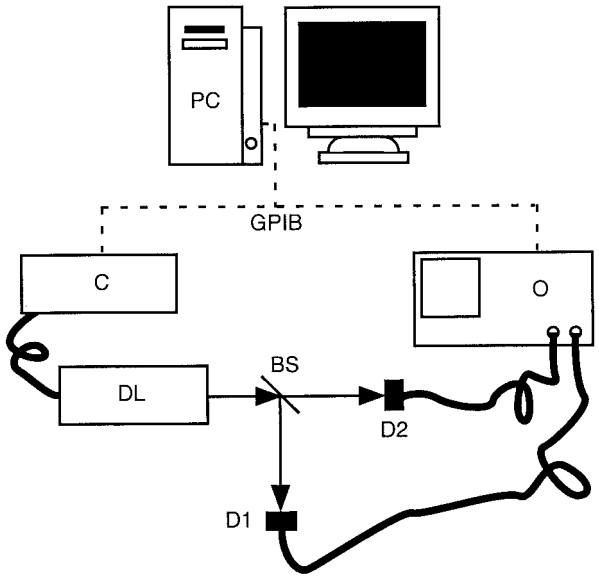

Fig. 5. Tunable infrared laser spectrophotometer system: C, controller for the diode laser; DL, tunable diode laser; BS, beam splitter; D1, D2, InGaAs photodetectors; O, digital oscilloscope; PC, digital computer with GPIB interface.

For these reasons we have developed a laser spectrophotometer system that features a coherent and collimated light source. This system is illustrated in Fig. 5. The light source is a tunable diode laser with a wavelength variable over the range 1469–1547 nm. The beam from the diode laser is split into two branches, a test arm and a reference arm. The intensity of the reference beam is measured by an InGaAs detector. The intensity of the test beam is measured by a second InGaAs detector after the beam first passes through the sample. The voltages from the two detectors are sent to a digital oscilloscope, which computes the ratio of the two signals. By recording this ratio as the laser wavelength is tuned, we trace the transmission through the sample as a function of wavelength. Finally, the transmission spectrum of the sample is normalized by the transmission spectrum of the test arm when the arm is empty. The system is calibrated with an acetylene absorption cell.[15]

3. Design Curves for Holographic Fabrication of Infrared Interference Filters

Having characterized the index of refraction, shrinkage, and sensitivity of the DuPont HRF-800X001 photopolymer, we were able to create design curves

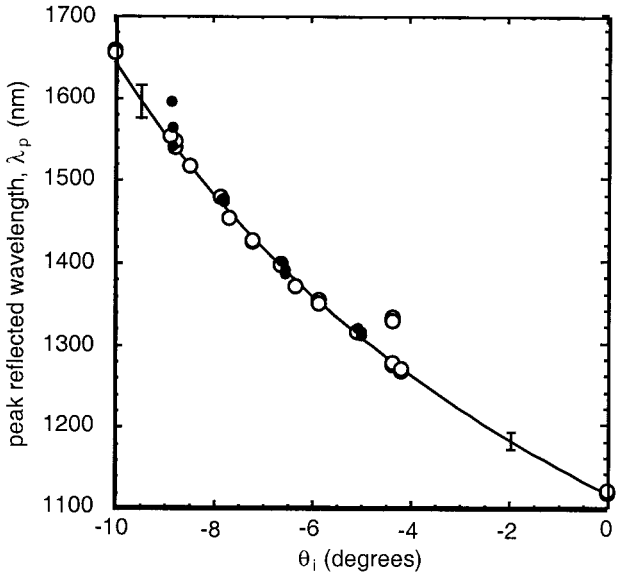

Fig. 6. Design curve relating exposure angle θ_i to peak reflected wavelength λ_p. Solid curve, plot of Eq. (4). The circles (filled and open) represent two sets of experimental data.

relating exposure angle θ_i to the resonant wavelength of the processed hologram, λ_p. The formula for this curve can be found by solution of Eqs. (1)–(3), with a reconstruction angle $\theta_f' = 0°$. The resulting relation is given by

$$\lambda = \lambda_0 S \frac{n_f'}{n_f}\left[1 - \frac{1}{2}\left(\frac{n_p}{n_f}\right)^2 + \frac{\sin\theta_i}{n_f^2} \times (n_p^2 - \sin^2\theta_i)^{1/2}\right]^{-1/2}. \quad (4)$$

A plot of this function is shown in Fig. 6. In evaluating this equation we used the average value of $n_f' = 1.485 \pm 0.005$, as described above. The plotted points represent the experimental data. The excellent agreement between the experimental data and the theoretical design curve demonstrates that our model is valid over the wavelength range indicated.

We then set out to construct design curves relating the efficiency and bandwidth of the filters to the thickness and index modulation of the film. In Subsection 3.A we explain the thin-film-decomposition technique in detail, and in Subsection 3.B we present the results of our calculations.

A. Thin-Film Decomposition

The central concept of thin-film decomposition is that an inhomogeneous multilayer film of arbitrary index profile $n(z)$ may be modeled as a stack of homogeneous layers. Within each layer the EM fields may be described as plane waves traveling through a material of constant index. By matching the boundary conditions between pairs of successive layers, one can ascertain the transmission and reflection properties of the film. One of the chief goals of this analysis is determination of the film transmission. These calculations are considerably streamlined by use of the chain-matrix formalism for multilayer films that was devised by Abeles.[22] As described in Section 1, the term "thin-film decomposition" was chosen in analogy to the nomenclature "thin grating decomposition."

In this paper we use the matrix notation found in Macleod's classic text, *Thin Film Optical Filters*.[23] Specifically, for a film layer of thickness d and index n upon a substrate with index n_s, the amplitudes of the electric and magnetic fields tangential to the air–film interface, a, and to the film–substrate interface, s, are related by the matrix equation

$$\begin{bmatrix} E_a \\ H_a \end{bmatrix} = \begin{bmatrix} \cos\delta & (i\sin\delta)/\eta \\ i\eta\sin\delta & \cos\delta \end{bmatrix}\begin{bmatrix} E_s \\ H_s \end{bmatrix}, \quad (5)$$

where δ is the phase thickness of the film and η is the optical admittance of the film. In general, δ and η are angle dependent, but for the special case of normal incidence they reduce to $\delta = 2\pi d/\lambda$, where λ is the wavelength of the incident light in vacuum and $\eta = n(\epsilon_0/\mu_0)^{1/2}$. Equation (5) is more useful when it is written in terms of indices of refraction rather than of electromagnetic fields. We can accomplish this transformation by noting that the substrate index, n_s, is given by the relation $n_s = (H_s/E_s)(\mu_0/\epsilon_0)^{1/2}$ and similarly by defining the effective index of the film–substrate composite as $n_a = (H_a/E_a)(\mu_0/\epsilon_0)^{1/2}$. Using these substitutions, we may write Eq. (5) as

$$\begin{bmatrix} B \\ C \end{bmatrix} = \begin{bmatrix} \cos\delta & (i\sin\delta)/n \\ in\sin\delta & \cos\delta \end{bmatrix}\begin{bmatrix} 1 \\ n_s \end{bmatrix}, \quad (6)$$

where $n_a = C/B$. The effective index of the film–substrate assembly, n_a, may then be used with the Fresnel relations to calculate the transmissivity and reflectivity of the film. It should be noted that, in general, n_a is complex and wavelength dependent. The matrix given in Eq. (6) is termed the characteristic matrix of the thin film and is denoted **M**. For a film consisting of more than one layer, one simply composes a characteristic matrix for each layer and then multiplies the matrices together to obtain a final matrix that is characteristic of the entire film.

For these calculations, we model the index within the film as a cosinusoidal variation given by the equation

$$n(z) = n_f' + \Delta n\cos\left(\frac{2\pi}{\Lambda}z\right), \quad (7)$$

where Δn represents the strength of the index modulation. In this case the index modulation is periodic, so the film can be divided into N identical cells (each one period thick) and a remainder. Once we have found the characteristic matrix for a single cell, we can find the characteristic matrix for the stack of N cells by self-multiplying the single cell matrix N times.

The first step in the decomposition process is to choose the thickness and the index for the homogeneous layers. Separate studies of the solution convergence were used to establish that $\Lambda/20$ is a

conservative choice for layer thickness and provides answers with accuracy surpassing the measurement capabilities of most spectrophotometers. We used the integrated average index of each slice of the inhomogeneous film as the index for the corresponding homogeneous layer. Once the index and the thickness of each layer have been determined, it is a simple matter to create the characteristic matrix for each layer by using Eq. (6). We find the characteristic matrices for the remainder and for a cell by multiplying the matrices of their constituent layers. As matrix multiplication is noncommutative, some care must be taken to multiply the matrices in the correct order; specifically, the matrix for the first illuminated layer is on the left, and all subsequent matrices follow on the right. To calculate the product of the identical characteristic matrices for the N cells, it is convenient to use an identity found in Born and Wolf's *Principles of Optics*.[24] Specifically, for a unimodular matrix $\mathbf{m}$, given by

$$\mathbf{m} = \begin{bmatrix} m_{11} & m_{12} \\ m_{21} & m_{22} \end{bmatrix}, \tag{8}$$

the Nth power of that matrix is

$$\mathbf{m}^N = \begin{bmatrix} m_{11}U_{N-1}(a) - U_{N-2}(a) & m_{12}U_{N-1}(a) \\ m_{21}U_{N-1}(a) & m_{22}U_{N-1}(a) - U_{N-2}(a) \end{bmatrix}, \tag{9}$$

where

$$a = \tfrac{1}{2}\,(m_{11} + m_{22}) \tag{10}$$

and U_N are the Chebyshev polynomials of the second kind:

$$U_N(a) = \frac{\sin[(N+1)\cos^{-1} a]}{(1-a)^{1/2}}. \tag{11}$$

By multiplying the characteristic matrix of the N cells by the characteristic matrix of the remainder, one ends up with a characteristic matrix that describes the entire film, denoted $\mathbf{M}_f$. Finally, one may find the effective index of the entire film–substrate assembly by plugging the characteristic matrix of the film, $\mathbf{M}_f$, into Eq. (6). The transmission through the film is given by the formula

$$T(\lambda) = \frac{4n_0\,\mathrm{Re}(n_s)}{(n_0 B + C)(n_0 B + C)^*}, \tag{12}$$

where n_0 is the index of the cover and the asterisk denotes the complex conjugate. For these calculations we assume that the cover and substrate indices are matched to the average index of the film (i.e., that $n_0 = n_s = n_f'$).

B. Design Curves for General Holographic Multilayers

As stated above, the purpose of carrying out these calculations has been to develop design curves to relate the efficiency and bandwidth of the holograms to the thickness and index modulation of the film. To this end, we used the thin-film-decomposition technique described above to compute the theoretical transmission spectra of a large ensemble of holograms. The index modulation, film thickness, and period were systematically varied in each of the calculations, and the spectra were evaluated to a precision of 1 nm over the range 1000–2000 nm. Afterward, the efficiencies and bandwidths of the spectra were measured, and the results analyzed.

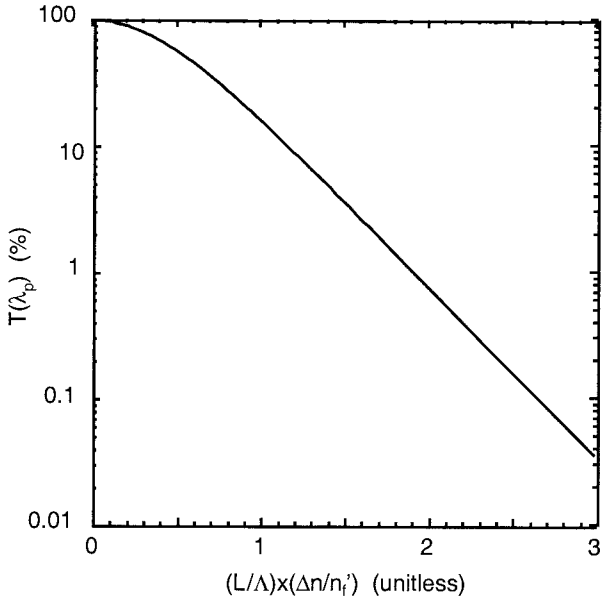

Fig. 7. Design curve plotting minimum transmission $T(\lambda_p)$ versus dimensionless parameter $(L/\Lambda) \times (\Delta n/n_f')$ for a cosinusoidal index variation. We calculated the curve by using thin-film decomposition.

Using the variable L to denote the thickness of the film, we found that, for holograms illuminated at optimal normal-incidence reconstruction wavelength λ_p, transmission efficiency $T(\lambda_p)$ decreased (i.e., reflection efficiency increased) in a smooth manner as a function of $(\Delta n/n_f') \times (L/\Lambda)$, as illustrated in Fig. 7. We observed that increasing either index modulation Δn or film thickness L has the same effect; that is, there can be a trade-off of index modulation for film thickness and vice versa.

We also created curves that revealed the interrelation between the FWHM bandwidth of the holographic multilayer, on the one hand, and the index modulation and film thickness, on the other, as shown in Fig. 8. For fixed thickness, bandwidth increases as index modulation increases. By contrast, for fixed index modulation, bandwidth decreases as thickness increases, seeming to approach an asymptotic limit dictated by the strength of the index modulation. These results demonstrate that film thickness and index modulation have different effects on the FWHM bandwidth of the hologram; that is, index modulation and film thickness cannot be traded for each other.

Using the design curve shown in Fig. 7, we deter-

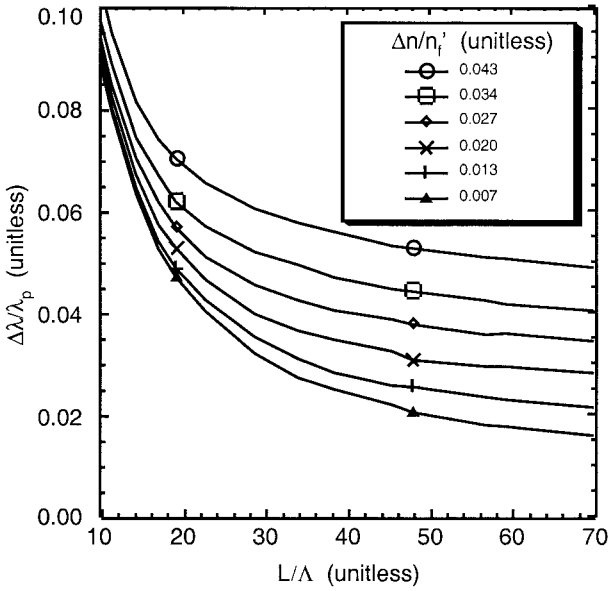

Fig. 8. Design curves for $\Delta\lambda/\lambda_p$ versus L/Λ, calculated by use of thin-film decomposition for a cosinusoidal index modulation and a range of index modulations characterized by $(\Delta n/n_f')$.

mined the size of the index modulation for the four example holograms whose transmission curves are shown in Fig. 3. The first hologram has a transmission minimum of 36.60% at 1311 nm; the second hologram has a transmission minimum of 39.57% at 1391 nm; the third hologram has a transmission minimum of 54.65% at 1473 nm; and the fourth hologram has a transmission minimum of 54.39% at 1541 nm. Using Fig. 7, we can see that these values correspond to values for $(\Delta n/n_f') \times (L/\Lambda)$ of $0.69\bar{8}$, $0.66\bar{6}$, $0.52\bar{7}$, and $0.52\bar{9}$, respectively. We know that the photopolymer has a final thickness (after shrinking) of $L = 14.625 \pm 0.045$ μm, and we can determine the period, Λ, by solving Eq. (2), given that $n_f' = 1.487 \pm 0.005$ and $\theta_f' = 0$ and that λ_p can be determined from the transmission spectrum of each hologram. Carrying out these calculations, we found the strength of the index modulation, Δn, for the four holograms to be 0.031, 0.032, 0.0265, and 0.028.

Conversely, the curves shown in Figs. 6–8 can be used in the design of a holographic filter. For example, if the desired replay wavelength, efficiency, and bandwidth are known, one can use Fig. 6 to determine the exposure angle and Figs. 7 and 8 to determine the proper thickness and index modulation for the hologram.

4. Summary

In this paper we have demonstrated a method for fabricating holographic interference filters for infrared applications by using a visible laser source and DuPont photopolymer film. The collimated laser illumination is coupled into the film at an oblique angle by use of a prism assembly, as illustrated in Fig. 1, and total internal reflection at the film–air interface creates the standing-wave interference pattern that is recorded within the film as index modulation.[2,3] By rotating the prism with respect to the incident beam, one can change the period of the final index modulation; thus the wavelength at which the hologram shows peak reflectivity at normal incidence will depend on the exposure angle. Figure 3 shows the transmission spectra for four such holograms, all recorded with the same exposure wavelength but each at a different exposure angle. With this exposure technique we created holograms with reflection peaks anywhere in the 1300–1600-nm range, by varying the exposure angle from 0° to −10°.

Using our experimental data, we determined that the index of refraction of the photopolymer in the near infrared is 1.485 ± 0.005. Combining this information with DuPont's published values for the index and shrinkage of the photopolymer at visible wavelengths,[12] we were able to generate a design curve that related the exposure angle to the peak reflection wavelength at normal incidence. The formula for this curve is given in Eq. (4), and the curve is traced in Fig. 6.

Finally, using thin-film decomposition, we have presented curves that relate the efficiency and bandwidth of the spectra to the thickness and index modulation of holograms with cosinusoidal index profiles as described in Eq. (7). These curves are shown in Figs. 7 and 8. Using these design curves, one may plan the exposure needed to create a holographic interference filter with a peak resonance at any desired wavelength, with any desired efficiency, and with any desired bandwidth. We stress that the thin-film-decomposition technique is valid for multilayer films of arbitrary index profile, not merely for periodic films.

We acknowledge the financial support of this project in part by the U.S. Army Research Office.

References

1. T. W. Stone and B. J. Thompson, eds., *Selected Papers on Holographic and Diffractive Lenses and Mirrors*, Vol. MS 34 of SPIE Milestones Series (SPIE Optical Engineering Press, Bellingham, Wash., 1991).
2. S. S. Duncan, J. A. McQuoid, and D. J. McCartney, "Holographic filters in dichromated gelatin position tuned over the near-infrared region," Opt. Eng. **24,** 781–785 (1985).
3. T. Stone, N. George, and B. D. Guenther, "Index variation and scattering in a holographic medium," in *Holographic Optics II: Principles and Applications*, G. M. Morris, ed., Proc. SPIE **1136,** 35–44 (1989).
4. R. Jacobsson, "Light reflection from films of continuously varying refractive index," in *Progress in Optics*, E. Wolf, ed. (North-Holland, Amsterdam, 1966), Vol. 5, Chap. 5, pp. 247–286.
5. D. H. Close, A. D. Jacobson, J. D. Margerum, R. G. Brault, and F. J. McClung, "Hologram recording on photopolymer materials," Appl. Phys. Lett. **14,** 159–160 (1969).
6. R. T. Ingwall and H. L. Fielding, "Hologram recording with a new photopolymer system," Opt. Eng. **24,** 808–811 (1985).
7. W. K. Smothers, T. J. Trout, A. M. Weber, and D. J. Mikish, "Hologram recording in DuPont's new photopolymer materials," in *Second International Conference on Holographic Systems, Components and Applications*, IEE Conf. Pub. **311,** 184–189 (1989).

8. J. L. Salter and M. F. Loeffler, "Comparison of dichromated gelatin and DuPont HRF-700 photopolymer as media for holographic notch filters," in *Computer and Optically Generated Holographic Optics*, I. Cindrich and S. H. Lee, eds., Proc. SPIE **1555,** 268–278 (1991).
9. L. T. Blair and L. Solymar, "Grating profiles in dichromated gelatin," Opt. Commun. **77,** 365–367 (1990).
10. T. J. Trout, W. J. Gambogi, and S. H. Stevenson, "Photopolymer materials for color holography," in *International Conference on Applications of Optical Holography*, T. Honda, ed., Proc. SPIE **2577,** 94–105 (1995).
11. K. W. Steijn, "Multicolor holographic recording in DuPont holographic recording film: determination of exposure conditions for color balance," in *Holographic Materials II*, T. J. Trout, ed., Proc. SPIE **2688,** 123–134 (1996).
12. S. H. Stevenson and K. W. Steijn, "A method for characterization of film thickness and refractive index in volume holographic materials," in *Holographic Materials*, T. J. Trout, ed., Proc. SPIE **2405,** 88–97 (1995).
13. H. J. Zhou, V. Morozov, and J. Neff, "Characterization of DuPont photopolymers in infrared light for free-space optical interconnects," Appl. Opt. **34,** 7457–7459 (1995).
14. A. Chen, Q. Gao, R. Fan, A. Harton, K. Wyatt, T. C. Felder, W. J. Gambogi, S. R. Mackara, K. W. Steijn, and T. J. Trout, "Enhanced reflective liquid crystal displays using DuPont holographic recording films," in *Holographic Materials IV*, T. J. Trout, ed., Proc. SPIE **3294,** 201–206 (1998).
15. K. Nakagawa, M. de Labachelerie, Y. Awaji, and M. Kourogi, "Accurate optical frequency atlas of the 1.5-μm bands of acetylene," J. Opt. Soc. Am. B **13,** 2708–2714 (1996).
16. M. G. Moharam and T. K. Gaylord, "Chain-matrix analysis of arbitrary-thickness dielectric reflection gratings," J. Opt. Soc. Am. **72,** 187–190 (1982).
17. X. Ning, "Analysis of multiplexed-reflection holographic gratings," J. Opt. Soc. Am. A **7,** 1436–1440 (1990).
18. R. Alferness, "Analysis of optical propagation in thick holographic gratings," Appl. Phys. **7,** 29–33 (1975).
19. R. Alferness, "Analysis of propagation at the second-order Bragg angle of a thick holographic grating," J. Opt. Soc. Am. **66,** 353–362 (1976).
20. T. W. Stone, "Holographic optical elements," Ph.D. dissertation (University of Rochester, Rochester, New York, 1986).
21. T. Stone and N. George, "Wavelength performance of holographic optical elements," Appl. Opt. **24,** 3797–3810 (1985).
22. P. F. Abeles, "Recherches sur la propagation des ondes électromagnétiques sinusoïdales dans le milieux stratifiés. Application aux couches minces," Ann. Phys. (Paris) **12,** 596–640, 706–784 (1950).
23. H. A. Macleod, *Thin-Film Optical Filters*, 2nd ed. (McGraw-Hill, New York, 1989).
24. M. Born and E. Wolf, *Principles of Optics: Electromagnetic Theory of Propagation, Interference and Diffraction of Light*, 7th ed. (Cambridge U. Press, Cambridge, 1999).